ACS Chemical Neuroscience

Letter

pubs.acs.org/chemneuro

Radiosynthesis and in Vivo Evaluation of Neuropeptide Y5 Receptor (NPY_5R) PET Tracers

J. S. Dileep Kumar,*[,†,∥] Mary Walker,[‡] Mathivanan Packiarajan,[‡] Vrej Jubian,[‡] Jaya Prabhakaran,[§] Gamini Chandrasena,[‡] Mali Pratap,[†] Ramin V. Parsey,[∥] and J. John Mann[†,§]

[†]Division of Molecular Imaging and Neuropathology, New York State Psychiatric Institute, New York, New York 10032, United States

[‡]Chemical & Pharmacokinetic Sciences and Synaptic Transmission, Disease Biological Unit, Lundbeck Research USA, Paramus, New Jersey 07652, United States

[§]Department of Psychiatry, Columbia University Medical Center, New York, New York 10032, United States

[∥]Department of Psychiatry and Behavioral Medicine, Stony Brook University, New York, New York 11794, United States

ABSTRACT: Neuropeptide Y receptor type 5 (NPY_5R) is a G-protein coupled receptor (GPCR) that belongs to the subfamily of neuropeptide receptors (NPYR) that mediate the action of endogenous neuropeptide Y (NPY). Animal models and preclinical studies indicate a role for NPY_5R in the pathophysiology of depression, anxiety, and obesity and as a target of potential therapeutic drugs. To better understand the pathophysiological involvement of NPY_5R, and to measure target occupancy by potential therapeutic drugs, it would be advantageous to measure NPY_5R binding in vivo by positron emission tomography (PET). Four potent and selective NPY_5R antagonists were radiolabeled via nucleophilic aromatic substitution reactions with [^{18}F]fluoride. Of the four radioligands investigated, PET studies in anesthetized baboons showed that [^{18}F]LuAE00654 ([^{18}F]*N*-[*trans*-4-({[4-(2-fluoropyridin-3-yl)thiazol-2-yl]amino}methyl)cyclohexyl]propane-2-sulfonamide) penetrates blood brain barrier (BBB) and a small amount is retained in the brain. Slow metabolism of [^{18}F]LuAE00654 was observed in baboon plasma. Blocking studies with a specific NPY_5R antagonist demonstrated up to 60% displacement of radioactivity in striatum, the brain region with highest NPY_5R binding. Our studies suggest that [^{18}F]LuAE00654 can be a potential PET radiotracer for the quantification and occupancy studies of NPY_5R drug candidates.

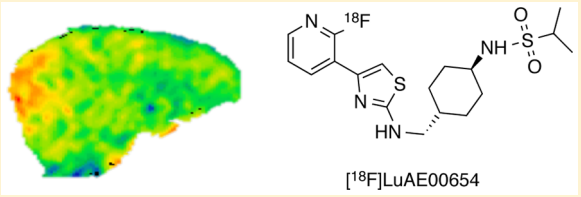

KEYWORDS: *Neuropeptide, brain, PET, antagonist, radiotracer*

Neuropeptide Y (NPY) is a 36 amino acid peptide originally discovered in porcine brain.[1] To date, five receptor subtypes, Y_1−Y_5, have been characterized and their signaling is mediated through Gi family of GPCRs.[2] NPY and its receptors are implicated in several disorders including obesity, major depression, and anxiety-related disorders.[3−9] Several brain structures are involved in mediating antistress actions of NPY, in particular striatum, amygdala, hippocampus, septum and locus coeruleus.[10] Antistress actions of NPY are mimicked by Y_1 receptor agonists, and blocked by Y_1 and Y_5 antagonists.[11] Together, available data point to the potential of the NPY system as a target for novel pharmacological treatments of stress-related disorders, including anxiety and depression.[12−15] NPY_5R antagonists reduce appetite in animal models with obesity and are being further optimized to identify clinical candidates for testing in human obesity.[16,17] Immunoprecipitation studies show that the NPY_5R is widely distributed in human brain, mostly in cortex, putamen and caudate nucleus.[18,19] To better understand the role of NPY_5R in pathologies and medication effects, it would be advantages to measure NPY_5R binding in vivo. PET imaging has been widely used to visualize brain receptors, to demonstrate target engagement by drug candidates, and to establish the receptor occupancy-response relationships to aid in dose-finding studies.[20] The radiosynthesis of several azaisobenzofuran derivatives that could act as NPY_5R PET agents are reported using [^{11}C]CO and palladium reagents.[21−23] Among these, [^{11}C]MK0233 has been studied in anesthetized monkeys and shows binding in striatum but with a low signal-to-noise ratio of less than two.[24] [^{11}C]MK0233 was also used for receptor occupancy studies in rhesus monkeys and human volunteers.[24,25] Lowest dose of MK0557, a selective NPY_5R antiobesity drug candidate exhibited 100% occupancy with [^{11}C]MK0233 in obese patients, however, the magnitude of weight loss was not clinically meaningful.[25] The failure of MK0557 as an obesity drug does not mean that drugs engaging this target may not be effective treatments for other disorders. Since NPY_5R target is relevant for the pathogenesis of several disorders and for that reason a PET tracer would be a valuable tool for studying those disorders. Herein we report the

Received: December 2, 2015
Accepted: February 17, 2016
Published: February 17, 2016

DOI: 10.1021/acschemneuro.5b00315
ACS Chem. Neurosci. 2016, 7, 540−545

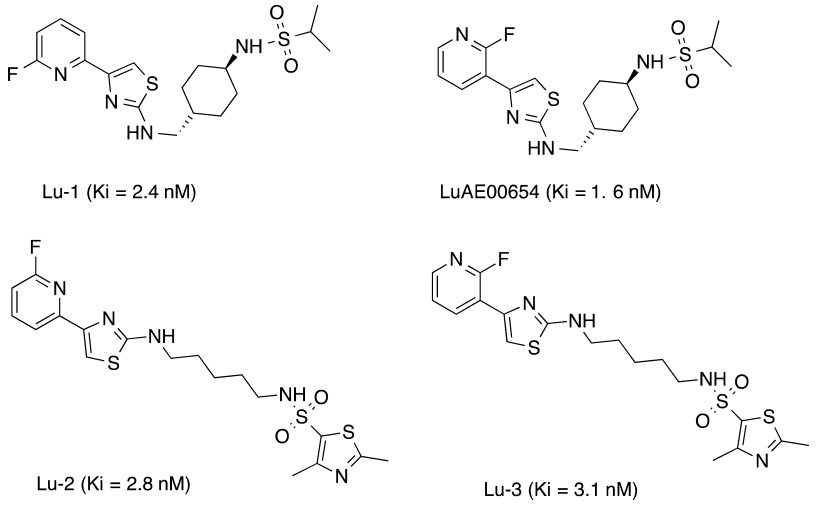

Figure 1. Candidate PET ligands for NPY_5R.

Scheme 1. Radiosynthesis of NPY_5R Ligands

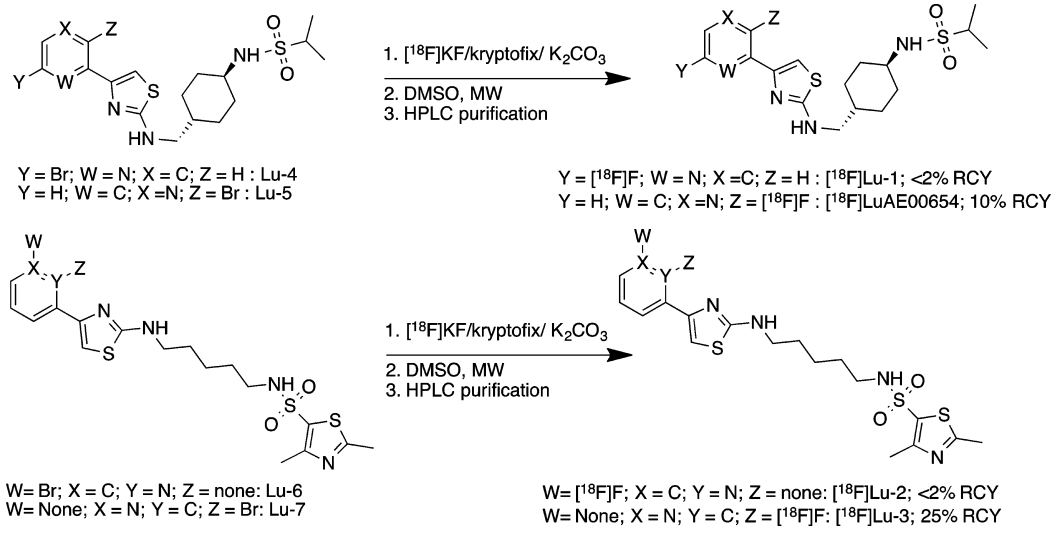

identification, radiolabeling and in vivo PET studies of potent and selective NPY_5R antagonists in nonhuman primates as promising PET imaging agents.

Four high affinity and selective NPY_5R antagonists amenable for radiolabeling via nucleophilic aromatic substitution reactions with [^{18}F]fluoride were selected as candidate radiotracers (Figure 1).[26,27] The nonradiolabeling experiments were performed using KF/kryptofix/K_2CO_3 at 180 °C in DMSO and established the formation of fluorinated products based on comparison with authentic standards using analytical HPLC. Under identical conditions, radiolabeling of the NPY_5R antagonist, Lu-1, did not provide any radiolabeled product. The radioproduct [^{18}F]Lu-1 was obtained in <2% isolated radiochemical yield (RCY) at the end of synthesis (EOS) under microwave irradiation in DMSO. The radiolabeling of 2-fluoropyridyl analogue [^{18}F]LuAE00654 was obtained in 10 ± 4% isolated RCY. The 6-fluoropyridyl ligand [^{18}F]Lu-2 did not undergo radiolabeling under thermal conditions, whereas under microwave irradiation conditions provided a <2% isolated RCY. The radiolabeling of 2-fluoropyridyl ligand [^{18}F]Lu-3 provided 25 ± 5% isolated RCY under microwave conditions and 15 ± 3% isolated RCY under conventional heating conditions (180 °C). The radiochemical purities of radiotracers are >95% with an average specific activity 2.5 ± 1 Ci/μmole. In general, 2-substituted pyridyl thiazoles provided better radiochemical yield in comparison to 6-substituted pyridyl thiazoles. Due to the poor radiochemical yield, further evaluations of [^{18}F]Lu-1 and [^{18}F]Lu-2 were not performed.

PET studies of [^{18}F]LuAE00654 and [^{18}F]Lu-3 were performed in fasted adult male baboons (*Papio anubis*) under anesthetic conditions. [^{18}F]LuAE00654 penetrated the BBB and shows retention in brain regions (Figure 2). Highest binding of [^{18}F]LuAE00654 was found in caudate, putamen, followed by cortical regions. Low binding was observed in hippocampus and thalamus, whereas, cerebellum showed the least binding of the radiotracer. The distribution of [^{18}F]-LuAE00654 is in agreement with the known distribution of NPY_5R and [^{11}C]MK0233 in monkeys and human subjects. Both tracers showed highest uptake in striatum and the lowest in cerebellum. Cortical regions and hippocampus showed relatively lower uptake.[24,25] The time activity curves (TACs) peaked by 0.25−5 min post injection of [^{18}F]LuAE00654 and demonstrated a rapid clearance of the tracer (Figure 3A).

Polar metabolites were observed in baboon plasma and the percentage of parent ligand was 94 ± 3.6% at 2 min, 84 ± 2.9% at 12 min, 84 ± 2.4% at 30 min, 79.6 ± 3.4% at 60 min, 72.3 ±

DOI: 10.1021/acschemneuro.5b00315
ACS Chem. Neurosci. 2016, 7, 540−545

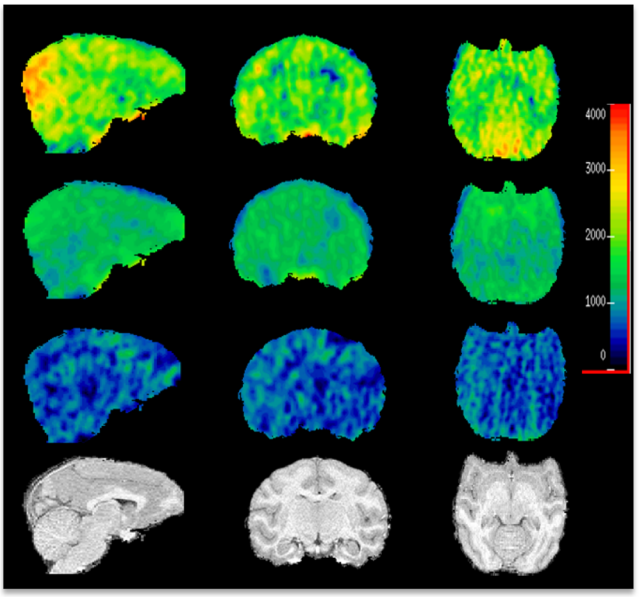

Figure 2. Sum of the mean PET images (0−120 min) of NPY_5R radioligands in a representative baboon scan. First row, PET images of [^{18}F]LuAE00654; second row, PET images of blocking experiment of [^{18}F]LuAE00654 with LuAA44608; third row, PET images of [^{18}F]Lu-3. First column, sagittal; second column, coronal; third column, transaxial.

5.5 at 90 min, and 66.6 ± 3.8% at 120 min respectively (Figure 3C). The free fraction (f_p) of the radiotracer was 1−3% based on ultracentrifuge assays.[28] Blocking experiments were performed with selective NPY_5R ligand LuAA44608 ($hNPY_5R$ K_i = 1.5 nM, and selectivity >2100-fold over >70 targets) (0.2 mg/kg, i.v.) 30 min prior to the administration of [^{18}F]LuAE00654 (Figure 3B). No significant changes of metabolism or protein binding were observed during blocking experiments with LuAA44608. A metabolite corrected arterial input function was used to determine the volume of distribution (V_T) of [^{18}F]LuAE00654 based on a two tissue compartment (2T) model.[29−31] A significant reduction of V_T was obtained for blocking experiments in comparison to baseline scans (Figure 4). Putamen and caudate regions show the highest specific binding expressed as V_T (60%) with respect to baseline and blocking experiments (Figure 4). Most cortical regions and cerebellum show 50−30% V_T changes. The least percentage of specific binding (10−15%) in terms of V_T changes was found in medial prefrontal cortex (MED), dorsal and lateral prefrontal cortex (DOR), prefrontal cortex (PFC), and hippocampus for [^{18}F]LuAE00654 after the blocking experiments.

We found [^{18}F]Lu-3 penetrate BBB in baboons (Figure 2, third row). However, TACs reveal very little retention of radioactivity in brain and a fast washout of the tracer (Figure 3D). [^{18}F]Lu-3 showed high protein binding (>98%) and metabolite analyses demonstrated rapid metabolism and evidence of polar metabolites in baboon plasma. The percentage of unmetabolized fractions of [^{18}F]Lu-3 were 83% at 2 min, 26% at 12 min, 18% at 30 min, 16% at 60 min, 15% at 90 min, and 12% at 120 min (Figure 2C). Our results also indicated that the metabolism of [^{18}F]Lu-3 was faster than that of [^{18}F]LuAE00654.

In summary, we synthesized four radioligands for NPY_5R. The radiosynthesis of 2-substituted pyridyl thiazoles [^{18}F]-LuAE00654 and [^{18}F]Lu3 provided better yield than the 6-substituted analogues [^{18}F]Lu1 and [^{18}F]Lu2. PET studies in anesthetized baboons show that [^{18}F]LuAE00654 penetrates the BBB and exhibits specific binding in NPY_5R enriched regions. The specificity of [^{18}F]LuAE00654 was demonstrated by blocking experiments using the known NPY_5R ligand LuAA44608. Although the proof of concept of in vivo imaging using [^{18}F]LuAE00654 is demonstrated in baboons, the radioligand showed small V_T for NPY_5R in comparison to the V_T values of radioligands for other well-established neuroreceptors. This may be partially attributed to the low concentration of NPY_5R in baboon brain. However, [^{18}F]-LuAE00654 may be a potential radioligand for occupancy measurements of novel drugs acting at NPY_5R in baboons or human subjects.

METHODS

General. The commercial chemicals and solvents used in the synthesis were purchased from Sigma-Aldrich Chemical Co. (St. Louis, MO), Fisher Scientific Inc. (Springfield, NJ), or Lancaster (Windham, NH) and were used without further purification. Analytical grade reagents were purchased from standard commercial sources. The reference standards and radiolabeling precursors were provided by Lundbeck Inc. HPLC analyses were performed using a Waters 1525 binary HPLC system (analytical: Phenomenex, Prodigy ODS(3) 4.6 × 250 mm, 5 μ column; semipreparative: Phenomenex, Prodigy ODS-prep 10× 250 mm, 10 μ column). Metabolite analyses were performed using Phenomenex Prodigy column (ODS3, 4.6 × 250 mm, 5 μ). The free fractions and metabolites were measured using Packard Instruments Gamma Counter (Model E5005, Downers Grove, IL). [^{18}F]fluoride was produced from RDS112 cyclotron (Siemens, Knoxville, TN). For detection of radiolabeled products, gamma ray detector (Bioscan Flow-Count fitted with a NaI detector) was used in series with the UV detector (Waters Model 996 set at 254 nm). Data acquisition for both the analytical and preparative systems was accomplished using a Waters Empower Chromatography System. PET studies were performed in baboon using an ECAT EXACT HR+ scanner (Siemens, Knoxville, TN). All animal experiments were carried out with the approval of the Institutional Animal Care and Use Committee of CUMC and NYSPI.

Radiochemistry. Aqueous solution of [^{18}F]fluoride (500 mCi to 1 Ci) generated from RDS 112 cyclotron was passed through an activated QMA and eluted with a mixture of K_2CO_3 (0.1 mL of 6 mg/mL water) and Kryptofix 222 (10 mg in 1 mL acetonitrile) in aqueous acetonitrile (1:10 v/v, 1 mL) into a clean 5 mL Reacti-vial. The amount of [^{18}F]fluoride collected was recorded and the solution was dried azeotropically with 3 × 0.5 mL of acetonitrile under a stream of argon at 110 °C. A solution of radiolabeling precursor (2−3 mg) in DMSO (0.5 mL) was added to the azeotropically dried [^{18}F]fluoride and the mixture was heated at 180 °C for 20 min or microwave irradiation for 5 min. The reaction mixture was allowed to cool, diluted with 50 mL deionized water, passed through a C-18 Sep-Pak cartridge (Waters), washed with 20 mL water to remove unreacted [^{18}F]fluoride and other polar impurities. The crude radioproduct was eluted with 1 mL of acetonitrile and injected on to a semipreparative RP-HPLC. The product fraction based on γ-detector was collected, diluted with 100 mL of deionized water, and passed through C-18 Sep-Pak cartridge (Waters). Reconstitution of the product in 1 mL of absolute ethanol afforded [^{18}F]NPY_5R radiotracers. [^{18}F]Lu-1 obtained in 2 ± 1 mCi (n = 4, <2% RCY) based on 500 ± 50 mCi of [^{18}F]fluoride using 45:55 v/v (acetonitrile/Na_2HPO_4 25 mM) as semipreparative mobile phase (retention time: ∼12 min). The corresponding analytical mobile phase was 50:50 v/v (acetonitrile/Na_2HPO_4 25 mM) (retention time: 8 min; synthetic time: 50 min). [^{18}F]LuAE00654 was obtained in 10 ± 4 mCi (n = 6, 10% RCY) based on 1 Ci ± 0.1 Ci of [^{18}F]fluoride using 40:50 v/v (acetonitrile/Na_2HPO_4 25 mM) as mobile phase for semipreparative HPLC purification (retention time: ∼ 14 min). The analytical HPLC mobile phase for [^{18}F]LuAE00654 was 40:50 v/v

DOI: 10.1021/acschemneuro.5b00315
ACS Chem. Neurosci. 2016, 7, 540−545

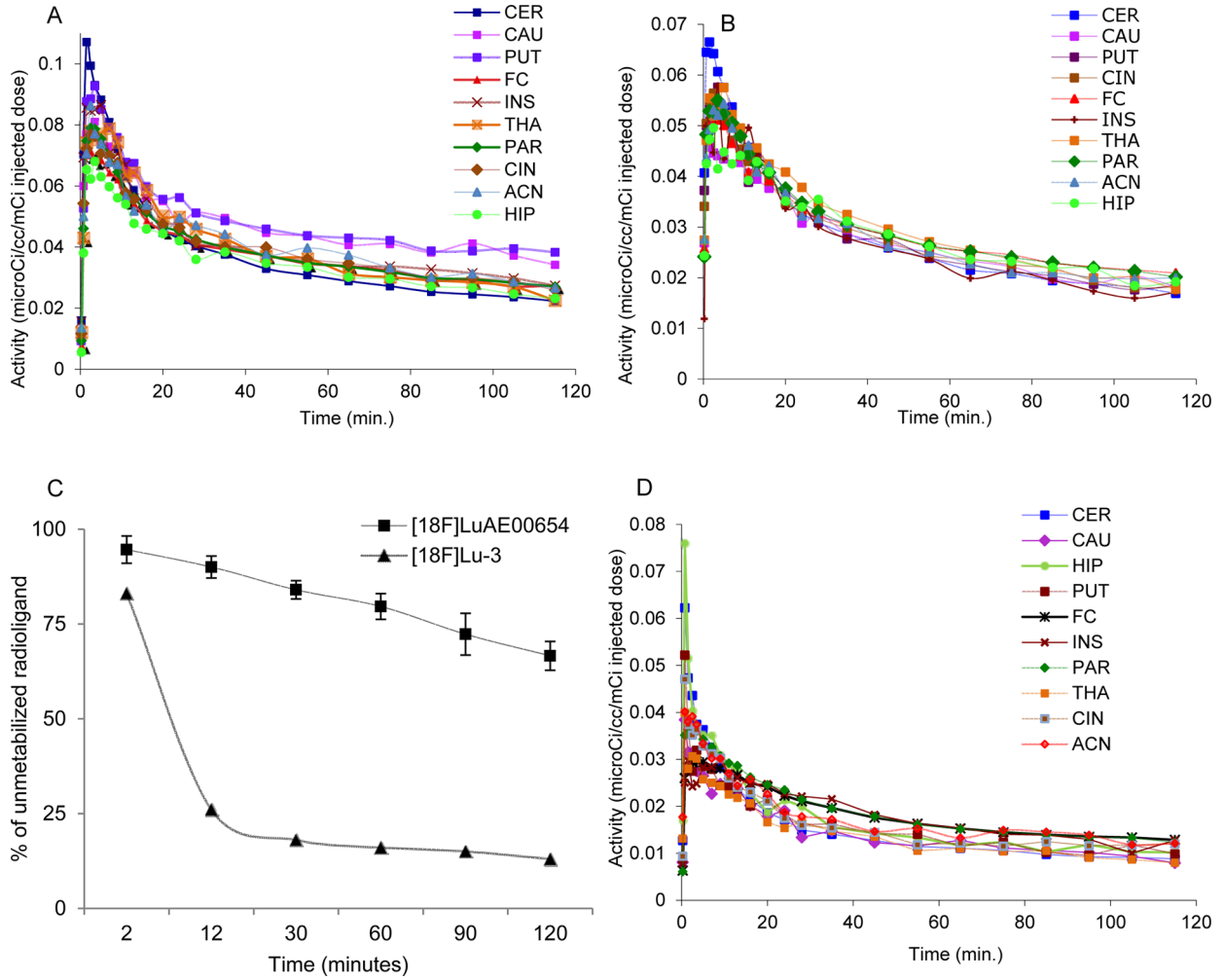

Figure 3. (A) TACs of [^{18}F]LuAE00654 in baboon brain. (B) TACs of [^{18}F]LuAE00654 in baboon brain after blocking with LuAA44608. (C) Percentages of unmetabolized [^{18}F]LuAE00654 and [^{18}F] Lu-3 in baboon plasma. (D) TACs of [^{18}F]Lu-3 in baboon brain (ACN, anterior cingulate; CAU, caudate; CER, cerebellum; CIN, cingulate cortex; FC, frontal cortex; HIP, hippocampus; INS, insular cortex; PUT:, putamen; PAR, parietal cortex; THA, thalamus).

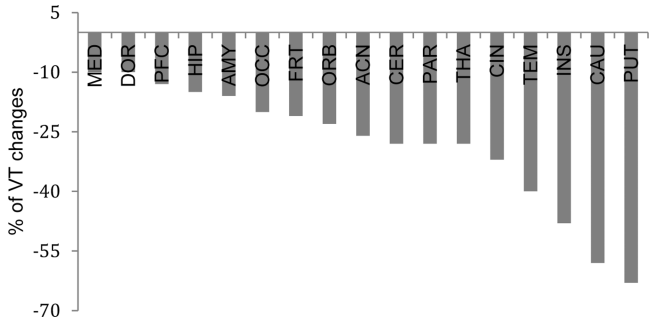

Figure 4. Percentages of total binding attributable to specific binding expressed as V_T of [^{18}F]LuAE00654 after the administration of the antagonist, LuAA44608, in baboon (AMY, amygdala; ACN, anterior cingulate; CER, cerebellum; CAU, caudate; CIN, cingulate cortex; DOR, dorsal and lateral prefrontal cortex; HIP, hippocampus; FRT, frontal cortex; MED, medial prefrontal cortex; OCC, occipital cortex; ORB, orbital cortex; PAR, parietal cortex; PUT:, putamen; TEM, temporal cortex; THA, thalamus).

(acetonitrile/Na_2HPO_4 25 mM) (retention time: 6 min; synthetic time: 60 min). The yield of [^{18}F]Lu-2 was 2 ± 0.5 mCi (n = 3, <1% RCY) starting with 500 ± 50 mCi of [^{18}F]fluoride using 40:60 v/v (acetonitrile/Na_2HPO_4 25 mM; semipreparative retention time: 8.5 min; analytical retention time: 7.2 min; synthetic time: 50 min) as mobile phase. [^{18}F]Lu-3 was obtained in 150 ± 25 mCi (n = 4, 25 ± 5% RCY) based on 1 ± 0.1 Ci of [^{18}F]fluoride using 40:60 v/v acetonitrile/Na_2HPO_4 25 mM as semipreparative HPLC mobile phase (retention time: 12 min). The analytical HPLC mobile phase for [^{18}F]Lu-3 was 50:50 v/v acetonitrile/Na_2HPO_4 25 mM (retention time: 5.5 min; synthesis time: 60 min). The semipreparative HPLC flow rates for all radiotracers were 10 mL/min and the corresponding analytical flow rates were 2 mL/min. The RCY reported are based on [^{18}F]KF/kryptofix/K_2CO_3 at EOS. A portion of the ethanol solution was analyzed by analytical HPLC to determine the specific activity, chemical and radiochemical purities. The specific activities were determined at EOS based on the UV absorption and concentration standard curves (λ = 254 nm). The remaining ethanol solution was diluted with 9 mL of normal saline and filtered through a 0.22 μm sterile filter into a sterile vial for further studies.

PET Studies in Baboons. PET scans were performed in two male baboons (22−25 kg) with an ECAT EXACT HR+ scanner (CPS/Knoxville, TN) as reported previously.[29] The fasted animal was immobilized with ketamine (10 mg/kg, i.m.) and anesthetized with 1.5−2.0% isoflurane via an endotracheal tube. Core temperature was kept constant at 37 °C with a heated water blanket. An intravenous infusion line with 0.9% NaCl was maintained during the experiment and used for hydration and radiotracer injection. An arterial line was placed for obtaining arterial samples for the input function. The head was positioned at center of the field of view, and a 10 min transmission

DOI: 10.1021/acschemneuro.5b00315
ACS Chem. Neurosci. 2016, 7, 540−545

scan was performed before the tracer injection. [^{18}F]NPY$_5$R radiotracers were injected (3 ± 0.5 mCi) as intravenous bolus over 30 s, and emission data were collected for 120 min in three-dimensional mode. Preadministration of NPY$_5$R selective antagonist LuAA44608 (0.2 mg/kg/i. v.) was performed 30−40 min prior to the tracer injection. Plasma samples were taken every 10 s for the first 2 min, using an automated system, and thereafter taken manually for a total of 34 samples.[29] Images were transferred into the image analysis software MEDx (Sensor Systems, Inc., Sterling, Virginia) for drawing and storing regions of interest. All PET images were coregistered within a dynamic study to the previous frame using the Functional Magnetic PET frames are then coregistered to the MRI using FLIRT.[29] All acquired frames were inspected to control for absence of head movements, and, coregistered to each other using the within modality registration software of Woods et al.[30] Frames were summed, and used to define the registration parameters with the MR image, then individual frames were registered to the MR data set based on the registration parameters of the summed PET image. Regions of interest drawn on the animal's MRI scan (custom shape) were transferred to coregistered automated image registration (AIR) frames of PET data.[29] Radioactivity levels in the right and left regions were averaged. Mean activities in the ROIs were determined as a function of TACs. Regional distribution volumes (V_T) of [^{18}F]LuAE00654 was derived from kinetic analysis using the arterial input function to derive the specific-to-nonspecific equilibrium partition coefficients based on a 2T model.[29,31,32] V_T (mL of plasma/g of tissue) is defined as the ratio of the tracer concentration in the region of interest to the metabolite-corrected plasma concentration of the tracer at equilibrium. Image analysis was performed in MATLAB (The Mathworks, Natick, MA) and statistical package for the social sciences (SPSS) software was used for statistical measurements. Brain activity was corrected for the contribution of plasma activity assuming a 5% blood volume in the ROIs.

Protein Binding and Metabolite Analyses. The protein binding of radiotracers in baboon blood samples were determined as described elsewhere.[28] The percentage of radioactivity in plasma as unchanged radiotracers were determined by HPLC.[29] Blood samples were taken at 2, 12, 30, 60, 90, and 120 min after radioactivity injection for metabolites analyses. The supernatant liquid obtained after centrifugation of the blood sample at 3400 rpm for 10 min was transferred (0.5 mL) into a tube and mixed with acetonitrile (0.7 mL). The resulting mixture was vortexed for 10 s, and centrifuged at 14 000 rpm for 4 min. The supernatant liquid (1 mL) was removed and the radioactivity was measured in a well-counter and the majority (0.8 mL) was subsequently injected onto the HPLC column equipped with a series radioactivity detector. The metabolite and free fractions were collected using a Bioscan gamma detector. All the acquired data were then subjected to correction for background radioactivity and physical decay to calculate the percentage of the parent compound in the plasma at different time points.

AUTHOR INFORMATION

Corresponding Author

*Tel: 646-774-7522. Fax: 646-774-7521. E-mail: kumardi@nyspi.columbia.edu.

Funding

This work was supported by a research grant from Lundbeck Research USA, Paramus, NJ.

Notes

The authors declare no competing financial interest.

REFERENCES

(1) Parker, E. M. (2004) Neuropeptide Y receptors. In *Encyclopedia of Biological Chemistry* (Lennarz, W. J., and Lane, M. D., Eds.), Vol. 3, pp 26−31, Elsevier, Amsterdam.

(2) DiBona, G. F. (2002) Neuropeptide Y. *Am. J. Physiol. 282* (3), R635−R636.

(3) Balasubramaniam, A. (2003) Neuropeptide Y (NPY) family of hormones: Progress in the development of receptor selective agonists and antagonists. *Curr. Pharm. Des. 9* (15), 1165−1175.

(4) Michel, M. C., Beck-Sickinger, A. G., Cox, H., Doods, H. N., Herzog, H., Larhammar, D., Quirion, R., Schwartz, T. W., and Westfall, T. C. (1998) XVI. International Union of Pharmacology recommendations for the nomenclature of neuropeptide Y, peptide YY and pancreatic polypeptide receptors. *Pharmacol. Rev. 50*, 143−150.

(5) Tatemoto, K. (2004) Neuropeptide Y: History and Overview. In *Handbook of Experimental Pharmacology 162* (Michel, M. C., Ed.), pp 2−15, Springer, New York.

(6) Thiele, T. E., Sparta, D. R., Hayes, D. M., and Fee, J. R. (2004) neuropeptide Y in neurobiological responses to ethanol and drugs of abuse. *Neuropeptides (Oxford, U. K.) 38* (4), 235−243.

(7) Moreno-Herrera, A., Garcia, A., Palos, I., and Rivera, G. (2014) Neuropeptide Y1 and Y5 Receptor Antagonists as Potential Anti-Obesity Drugs: Current Status. *Mini-Rev. Med. Chem. 14* (11), 896−919.

(8) Redrobe, J. P., Carvajal, C., Kask, A., Dumont, Y., and Quirion, R. (2004) Neuropeptide Y and its receptor subtypes in the central nervous system: emphasis on their role in animal models of psychiatric disorders. *Handb. Exp. Pharmacol. 162*, 101−136.

(9) Redrobe, J. P., Dumont, Y., and Quirion, R. (2002) Neuropeptide Y (NPY) and depression: From animal studies to the human condition. *Life Sci. 71*, 2921−2937.

(10) Mori, R. C., Telles, M. M., Guimaraes, R. B., Novo, N. F., Juliano, Y., Nascimento, C. M. O., and Ribeiro, E. B. (2004) Feeding Induced by Increasing Doses of Neuropeptide Y: Dual Effect on Hypothalamic Serotonin Release in Normal Rats. *Nutr. Neurosci. 7*, 235−239.

(11) Carvajal, C. C., Vercauteren, F., Dumont, Y., Michalkiewicz, M., and Quirion, R. I. (2004) Aged neuropeptide Y transgenic rats are resistant to acute stress but maintain spatial and non-spatial learning. *Behav. Brain Res. 153* (2), 471−480.

(12) Heilig, M., and Thorsell, A. (2002) Brain neuropeptide Y (NPY) in stress and alcohol dependence. *Rev. Neurosci. 13*, 85−94.

(13) Brothers, S. P., and Wahlestedt, C. (2010) Therapeutic potential of neuropeptide Y (NPY) receptor ligands. *EMBO Mol. Med. 2* (11), 429−439.

(14) Heilig, M. (2004) The NPY system in stress, anxiety and depression. *Neuropeptides 38*, 213−224.

(15) Heilig, M. (2004) Brain neuropeptide Y (NPY) system: a candidate target for treatment of anxiety, depression and alcohol dependence. *Drugs Future 29*, 137−147.

(16) Kaga, T., and Inui, A. (2000) Neuropeptide Y and its receptors in the regulation of feeding and body weight. *Horumon to Rinsho 48*, 1091−1099.

(17) Criscione, L., Rigollier, P., Batzl-Hartmann, H. C., Rueger, H., Stricker-Krongrad, K. A., Wyss, P., Brunner, L., Whitebread, S., Yamaguchi, Y., Gerald, C., Heurich, R. O., Walker, M. W., Chiesi, M., Schilling, W., Hofbauer, K. G., and Levens, N. (1998) Food intake in free-feeding and energy-deprived lean rats is mediated by the neuropeptide Y5 receptor. *J. Clin. Invest. 102*, 2136−2145.

(18) Dumont, Y., Jacques, D., Bouchard, P., and Quirion, R. (1998) Species differences in the expression and distribution of the neuropeptide Y Y1, Y2, Y4, and Y5 receptors in rodents, guinea pig, and primates brains. *J. Comp. Neurol. 402* (3), 372−384.

(19) Jacques, D., Tong, Y., Shen, S. H., and Quirion, R. (1998) Discrete distribution of the neuropeptide Y Y5 receptor gene in the human brain: an in situ hybridization study. *Mol. Brain Res. 61* (1−2), 100−107.

(20) Zhang, y., and Fox, G. B. (2012) PET imaging for receptor occupancy: meditations on calculation and simplification. *J. Biomed. Res. 26* (2), 69−76.

(21) Burns, D. H., Gibson, R. E., Hamill, T. G., and Kukami, T. (2004) Radiolabeled neuropeptide Y Y5 receptor anatagonists. U.S Patent 0192705.

(22) Takahashi, H., Haga, Y., Shibata, T., Nonoshita, K., Sakamoto, T., Moriya, M., Ohe, T., Chiba, M., Mitobe, Y., Kitazawa, H., Iwaasa,

DOI: 10.1021/acschemneuro.5b00315
ACS Chem. Neurosci. 2016, 7, 540−545

H., Ishihara, A., Ishii, Y., Kanatani, A., and Fukami, T. (2009) Identification of positron emission tomography ligands for NPY Y5 receptors in the brain. *Bioorg. Med. Chem. Lett. 19* (18), 5436−9.
(23) Kealey, S., Plisson, C., Collier, T. L., Long, N. J., Husbands, S. M., Martarello, L., and Gee, A. D. (2011) Microfluidic reactions using [11C]carbon monoxide solutions for the synthesis of a positron emission tomography radiotracer. *Org. Biomol. Chem. 9* (9), 3313−3319.
(24) Hostetler, E., Sanabria, S., Krause, S., Ryan, C., Francis, B., Eng, W. S., Hargreaves, R., and Burns, D. (2006) Neuropeptide-Y Y5 (NPY5) receptor: Occupancy studies in Rhesus monkey using a novel NPY5PET tracer. *NeuroImage 31*, T16.
(25) Erondu, N., Gantz, I., Musser, B., Suryawanshi, S., Mallick, M., Addy, C., Cote, J., Bray, G., Fujioka, K., Bays, H., Hollander, P., Sanabria-Bohorquez, S. M., Eng, W., Langstrom, B., Hargreaves, R. J., Burns, D. H., Kanatani, A., Fukami, T., MacNeil, D. J., Gottesdiener, K. M., Amatruda, J. M., and Kaufman, K. D. (2006) Neuropeptide Y5 receptor antagonism does not induce clinically meaningful weight loss in overweight and obese adults. *Cell Metab. 4*, 275−282.
(26) Packiarajan, M., Marzabadi, M. R., Desai, M., Lu, Y., Noble, S. A., Wong, W. C., Jubian, V., Chandrasena, G., Wolinsky, T. D., Zhong, H., and Walker, M. W. (2011) Discovery of Lu AA33810: A highly selective and potent NPY5 antagonist with in vivo efficacy in a model of mood disorder. *Bioorg. Med. Chem. Lett. 21* (18), 5436−5441.
(27) Packiarajan, M., Coate, H., Desai, M., Jimenez, M. N., Reinhard, E. J., Jubian, V. J., Marzabadi, M. R., Chandrasena, G., Wolinski, T. C., Walker, M. W., and Andersen, K. (2011) 5-(2′-Pyridyl)-2-amino-thiazoles: Alkyl amino sulfonamides and sulfamides as potent NPY5 antagonists. *Bioorg. Med. Chem. Lett. 21* (21), 6500−6504.
(28) Gandelman, M. S., Baldwin, R. M., Zoghbi, S. S., Zea-Ponce, Y., and Innis, R. B. (1994) Evaluation of ultrafiltration for the free-fraction determination of single photon emission computed tomography (SPECT) radiotracers beta-CIT, IBF, and iomazenil. *J. Pharm. Sci. 83*, 1014−1019.
(29) Kumar, J. S. D., Majo, V. J., Tamir, H., Milak, M. S., Hsing, S.-C., Prabhakaran, J., Simpson, N. R., Van Heertum, R. L., Mann, J. J., and Parsey, R. V. (2006) Synthesis and *in vivo* validation of [^{11}C]MPT: A potential 5-HT$_{1A}$ receptor agonist PET ligand. *J. Med. Chem. 49*, 125−134.
(30) Woods, R. P., Grafton, S. T., Holmes, C. J., Cherry, S. R., and Mazziotta, J. C. (1998) Automated image registration: I. General methods and intrasubject, intramodality validation. *J. Comput. Assist. Tomogr. 22*, 139−52.
(31) Parsey, R. V., Slifstein, M., Hwang, D.-R., Abi-Dargham, A., Simpson, N., Mawlawi, O., Guo, N.-N., Van Heertum, R., Mann, J. J., and Laruelle, M. (2000) Validation and reproducibility of measurement of 5-HT1A receptor parameters with [carbonyl-11C]WAY-100635 in humans: Comparison of arterial and reference tissue input functions. *J. Cereb. Blood Flow Metab. 20*, 1111−1133.
(32) Mintun, M. A., Raichle, M. E., Kilbourn, M. R., Wooten, G. F., and Welch, M. J. (1984) A quantitative model for the in vivo assessment of drug binding sites with positron emission tomography. *Ann. Neurol. 15*, 217−227.

DOI: 10.1021/acschemneuro.5b00315
ACS Chem. Neurosci. 2016, 7, 540−545